American Mineralogist, Volume 62, pages 438–448, 1977

Distribution of titanium between coexisting muscovite and biotite in pelitic schists from northwestern Maine

CHARLES V. GUIDOTTI, JOHN T. CHENEY[1] AND STEPHEN GUGGENHEIM[2]

Department of Geology and Geophysics
University of Wisconsin, Madison, Wisconsin 53706

Abstract

Data are presented bearing on (1) variation of Ti in coexisting muscovite and biotite as a function of metamorphic grade, and (2) variation of K_D, Ti $\frac{Mu}{Bio}$ (designated by the abbreviation, K_D) as a function of metamorphic grade and Mg/Fe ratio of the biotite. All specimens are from pelitic schists of northwestern Maine and have been chosen so that all are saturated with respect to Al, Si, and Ti. Moreover, the presence of graphite indicates that Fe is predominately in the ferrous state.

Within the context of these boundary conditions it is shown that: (1) Ti increases in both muscovite and biotite with increased grade due to expansion of the Ti saturation limit; (2) K_D may increase slightly over the range from the staurolite to the upper sillimanite grade of metamorphism; (3) at a given grade of metamorphism the Ti content of biotite decreases as its Mg/Fe ratio increases. As a result, K_D shows a marked increase in such specimens.

Typically, biotites with high Mg/Fe ratio have less Ti but more Si (less Al^{IV}). A model is proposed suggesting that the variations of Ti, Si and Al^{IV} associated with increase of Mg/Fe represent a mechanism for maintaining a dimensional fit of the tetrahedral and octahedral sheets. Such a mechanism would lessen the amount of tetrahedral rotation (α) otherwise required to achieve this dimensional fit.

Introduction

Electron microprobe analysis of muscovite and biotite from pelitic schists in northwestern Maine has provided data on the variation of Ti content in these minerals as a function of metamorphic grade and mineral assemblage. Chemical analyses, specific locations of specimens, and petrographic descriptions are given in Evans and Guidotti (1966), Guidotti (1970, 1974), Guidotti *et al.* (1975a,b), and Cheney (1975).

This paper considers only Al-saturated biotite and muscovite, in most cases from specimens with limiting assemblages, *i.e.* assemblages in which the number of phases present equals the number of components required to describe the phases, and hence phase compositions are a function of the intensive variables (Albee, 1965). In this context the following are considered: (a) the Ti content of muscovite and biotite as a function of metamorphic grade, (b) the distribution of Ti between coexisting muscovite and biotite as a function of grade, and (c) the influence of biotite Mg/Fe ratio on the Ti content of biotite and hence on K_D. Topics (a) and (b) have been considered previously (see references in Guidotti, 1970). Although consideration of topic (c) appears to be new, the reverse relationship (*i.e.*, the influence of Ti on biotite Mg/Fe ratio) has been discussed previously (*e.g.*, Dallmeyer, 1974a,b; Dahl, 1970).

Because all specimens are also saturated with respect to SiO_2 and TiO_2 (quartz and ilmenite or rutile are always present), they are ideal for investigating some of the crystallochemical implications of Mg–Fe substitution. This is especially so because the bulk compositions of the rocks span a rather wide range of MgO/FeO ratio. Guidotti *et al.* (1975b) have already shown that over much of the Mg–Fe range of the biotite composition field the amount of Al^{VI} is independent of Mg/Fe. Moreover, the presence of graphite in virtually all samples and the total absence of hematite and magnetite suggest that iron is predominantly in the ferrous state. Hence, we can assume that Fe^{3+} contents are minimal and uniform in all minerals.

[1] Present address: Department of Geology, Amherst College, Amherst, Massachusetts 01002.

[2] Present address: Department of Geological Sciences, University of Illinois at Chicago, Chicago, Illinois 60680.

Petrologic setting

The specimens are from portions of the Oquossoc, Rangeley, Old Speck Mountain, and Bryant Pond 15′ quadrangles in northwestern Maine, and formed in grades ranging from the staurolite zone to the K-feldspar+sillimanite zone (see references above). The pertinent data can be summarized according to grade and location as follows (all assemblages contain Mu + Pl + Qz[3]):

(a) *Upper staurolite zone:* North-central and south-central portions of the Rumford and Rangeley quadrangles respectively. High-alumina, limiting assemblages include: St + Gn + Bio + Chl + Il ± Po ± Grp; Crd + Bio + Chl + Ru + Po + Grp.

(b) *Transition zone:* Southwestern portion of the Rangeley quadrangle. High-alumina, limiting assemblages include: Si + St + Gn + Bio ± Chl + Il ± Po ± Grp.

(c) *Lower sillimanite zone:* Southwestern and north-central portions of the Rangeley and Rumford quadrangles respectively. High-alumina, limiting assemblages include: Si + St + Gn + Bio + Il ± Po ± Grp; Crd + Bio + Chl + Ru + Po + Grp.

(d) *Lower sillimanite zone:* Southeastern portion of the Oquossoc quardrangle. High-alumina, limiting assemblages include: Si + St + Gn + Bio + Il ± Po ± Grp.

The following are not true limiting assemblages, but this causes no difficulties for the purposes of this paper because the assemblages are still Al-saturated:

(e) *Upper sillimanite zone:* Southeastern portion of the Oquossoc quadrangle. High-alumina assemblages include: Si + Gn + Bio + Il ± Po ± Grp.

(f) *Upper sillimanite zone:* Bryant Pond quadrangle, southeastern portion of the Old Speck Mountain quadrangle, and southern portion of the Rumford quadrangle. High-alumina assemblages include: Si ± Gn + Bio ± Il ± Ru ± Po ± Grp.

(g) *K-feldspar + sillimanite zone:* Bryant Pond quadrangle. High alumina assemblages include: Si + Bio ± Gn ± Ksp ± Il ± Grp.

Groups (a) to (e) are from contiguous zones and represent a progressive metamorphic sequence. Group (b), the transition zone as defined by Guidotti (1974), represents a facies transitional between Groups (a) and (c) because it is a mappable zone which contains mineralogic aspects (Si + Chl) common to the zones above and below it. Groups (f) and (g) are contiguous zones but are separated by about 20 km from Groups (a)-(e). Moreover, Group (f) probably lies at higher grade in the upper sillimanite zone than does Group (e).

[3] Mineral abbreviations as follows: Mu, muscovite; Chl, chlorite; Bio, biotite; St, staurolite; Si, sillimanite; Gn, garnet; Il, ilmenite; Crd, cordierite; Qz, quartz; Pl, plagioclase; Po, pyrrhotite; Grp, graphite; Adl, andalusite; Ksp, K-feldspar; Ru, rutile.

Table 1. Average values for the distribution of Ti between coexisting muscovite and biotite in relation to Mg/Fe biotite and the Mg/Fe distribution coefficient for muscovite and biotite, Data for individual specimens is given in Tables 2A-2I (see footnote, page 440).

Grade	(5)Wt% Ti Mu	Wt% Ti Bio	$\frac{\text{Ti Mu}}{\text{Ti Bio}}$	Mg/Fe Bio	Mg/Fe Musc	$\frac{\text{Mg/Fe Mus}}{\text{Mg/Fe Bio}}$	Table
U.St.Z. (Ra)(6)	.22	.97	.224	.859	1.085	1.265	2A (18 spec.)
Tr.Z. (Ra)	.26	1.02	.255	.874	1.103	1.277	2B (12 spec.)
Low Si.Z. (Ra)	.30	1.08	.282	.822	1.251	1.519	2C (10 spec.)
Low Si.Z. (Oq)	.31	1.15	.274	.672	1.014	1.513	2E (14 spec.)
U.Si.Z. (Oq)	.42	1.38	.307	.698	1.061	1.506	2F (14 spec.)
U.Si.Z. (BP)	.42	1.48	.280	.770	1.009	1.331	2G (9 spec.)
Ksp.+Si.Z. (BP)	.59	1.94	.303	.690	.922	1.339	2I (12 spec.)
Sm.F. (N.Rum)	.32	.45	.764	6.455	6.463	1.051	2D (8 spec.)
Sm.F. (S.Rum)	.62	.78	.840	4.002	3.769	.924	2H (6 spec.)

(5) The analytical error for data in this and all subsequent tables is about two percent for elements constituting more than two percent of a given specimen. For elements analyzed together (Fe, Mg, Ti) the relative amounts have a similar error even for lower concentrations.

(6) U.St.Z. (Ra) = Upper staurolite zone, Rangeley Quad.; Tr.Z. = Transition zone, Rangeley Quad.; Low Si.Z. (Ra) = Lower sillimanite zone, Rangeley Quad.; Low Si.Z. (Oq) = Lower sillimanite zone, Oquossoc Quad.; U.Si.Z. (Oq) = Upper sillimanite zone, Oquossoc Quad.; U.Si.Z. (BP) = Upper sillimanite zone, Bryant Pond Quad.; Ksp. + Si.Z. (BP) = K-feldspar + sillimanite zone, Bryant Pond Quad.; Sm.F. (N.Rum) = sulfide-rich, Small's Falls specimens, Staurolite to Lower sillimanite zone, northern Rumford Quad.; Sm.F. (S. Rum) = sulfide-rich, Small's Falls specimens, Upper sillimanite zone, southern Rumford Quad.

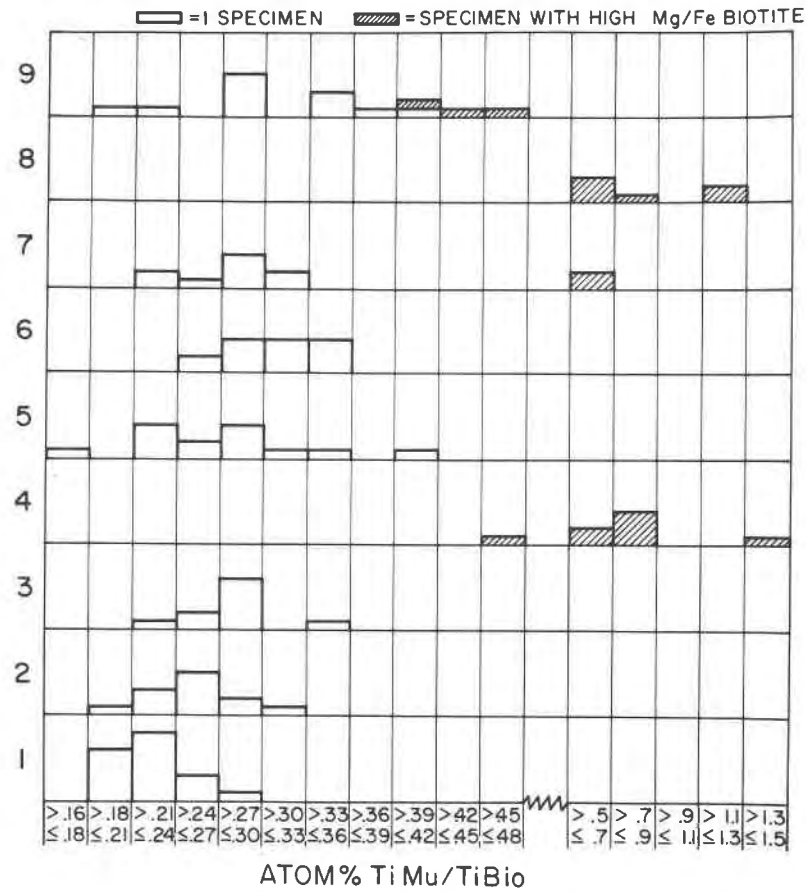

Fig. 1. Histograms showing variation of Ti Mu/Ti Bio as a function of metamorphic grade. Numbers 1–9 on the left margin of the diagram refer to data taken from tables 2A–2I respectively.

Analytical results

Table 1 summarizes the important analytical data for the different groups of specimens. Tables 2A–2I[4] present the same data for the individual specimens in each group. Excluding specimens from the very sulfide-rich Small's Falls Formation, Table 1 shows that the average weight-percent of Ti in muscovite from high-alumina, limiting assemblages increases from 0.22 to 0.59 from the upper staurolite zone to the K–feldspar + sillimanite zone, whereas for biotite the change is from 0.97 to 1.94 weight percent. Figure 1 shows that there may be some tendency for K_D to increase with grade from the staurolite to sillimanite zone (excluding specimens from the Small's Falls Formation), but the change is insignificant in higher-grade rocks. Kwak (1968) has reported a similar variation of K_D in staurolite and sillimanite grade rocks.

Table 1 shows that the Ti content of biotite decreases with increasing Mg/Fe in the biotite (*e.g.*, compare the data from Tables 2A–2C with that from Table 2D). However, in the coexisting muscovite, Ti changes little or possibly increases slightly. Hence, as shown in Figure 2, a correlation exists between high Mg/Fe ratio of biotite and high K_D.

The slight trend for Ti enrichment in muscovite from specimens with Mg-rich biotite might conceivably lead one to ascribe the change of K_D to some aspect of muscovite rather than biotite. However, it appears that variation of Ti in biotite as a function of biotite Mg/Fe ratio is much more important. The data tabulated in Tables 2A–2I show a *marked* decrease of Ti in Mg-rich biotites. This relationship is emphasized by Tables 3A and 3B, which compare staurolite zone to lower sillimanite zone, high Mg/Fe biotites versus those with only moderate Mg/Fe ra-

[4] To receive copies of Tables 2A–2I, order document Am–77–043 from the Business Office, Mineralogical Society of America, Suite 1000 lower level, 1909 K Street, N.W., Washington D.C. 20006. Please remit $1.00 for the microfiche.

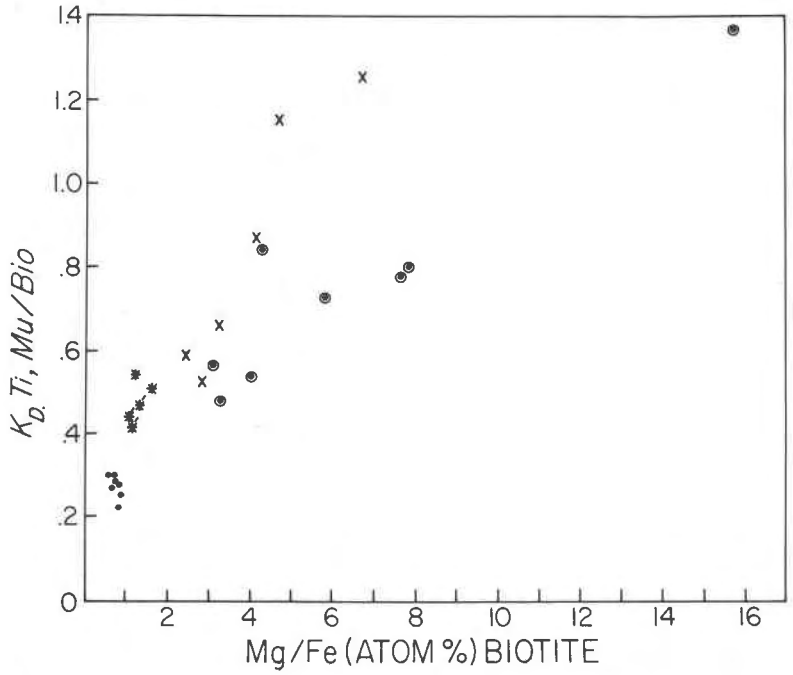

Fig. 2. Plot of K_D, Ti, Mu/Bio *vs.* Mg/Fe of biotite.
• = Average values for Upper Staurolite Zone through K-feldspar + Sillimanite Zone. Data from Tables 2A, 2B, 2C, 2E, 2F, 2G, and 2I (excluding specimens with an asterisk). Specimens with an asterisk have high Mg/Fe ratio in biotite and are plotted separately (see below).
⊙ = Specimens from the Small's Falls Formation in the Staurolite to Lower Sillimanite Zone.
× = Specimens from the Small's Falls Formation in the Upper Sillimanite Zone.
* = Specimens from Table 2G (Upper Sillimanite Zone) with high Mg/Fe ratio in biotite.
*′ = Specimens from Table 2I (K-feldspar + Sillimanite Zone) with high Mg/Fe ratio in biotite.

tio. The change of Ti content from one group of biotites to the other is obvious. On the other hand, the muscovites which coexist with the biotites listed in Tables 3A and 3B show little or no difference with respect to Ti content, despite a radical change in the Mg/Fe ratio [but not Σ(Fe + Mg)]. Although increase in Ti in muscovite from rocks with high biotite Mg/Fe ratio may contribute to the increase of K_D for such specimens, it appears much more likely that the increase of K_D is caused by the decrease of Ti in biotite. High Mg-content in biotite apparently inhibits its substitution by Ti—at least by comparison with Mg-poorer biotites. This statement is made only with respect to Al-saturated biotites.

Figure 3 is a plot of Mg/Fe *vs.* Ti for the biotites listed in Tables 3a, B, C. Besides showing the inverse relation between Mg/Fe and Ti, this diagram also calls attention to the change of the Ti-saturating phase (rutile) in the specimens with Mg-rich biotite. The existence of two parallel plots for specimens with rutile as the Ti-saturating phase is the result of difference in metamorphic grade. Figure 4 shows schematically a possible representation of how the biotite solid-solution field with respect to Ti changes as a function of biotite Mg/Fe ratio and the Ti-saturating phase. More complete biotite data will be required to ascertain accurately the shape or limits of the biotite solid-solution field with respect to Ti. Although the Ti saturation limit shrinks for biotite coexisting with rutile, reasons are presented below which strongly suggest a relatively greater availability of Ti for the micas in such specimens.

Discussion

The analytical data exhibit three general relationships deserving of discussion. These are: (1) the absolute increase of Ti in the two micas as a function of grade, (2) the possibility of a small change of K_D as a function of metamorphic grade from the staurolite zone to the sillimanite zone, and (3) the inverse relationship between K_D and biotite Mg/Fe ratio. In all

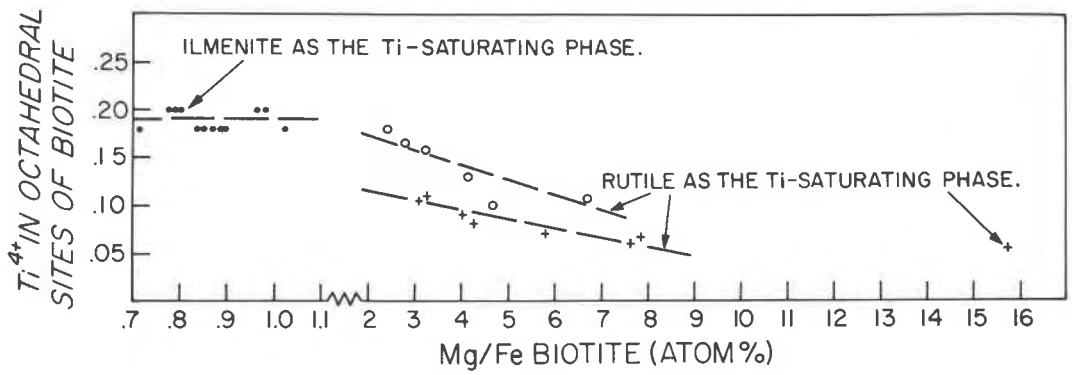

Fig. 3. Plot of Ti in the formula unit of biotite *vs.* Mg/Fe ratio of biotite.
• = Biotites from the Staurolite to Lower Sillimanite Zone, Rangeley Quadrangle. Data from Table 3A.
+ = Biotites from the Staurolite to Lower Sillimanite Zone in the Small's Falls Formation, northern portion of the Rumford Quadrangle. Data from Table 3B.
O = Biotites from the Upper Sillimanite Zone in the Small's Falls Formation. Southwest portion of the Rumford Quadrangle. Data from Table 3C.

of the following discussion it is assumed that Ti is tetravalent and substitutes into octahedral sites.

(1) Absolute increase of Ti in the micas as a function of grade

Inasmuch as all specimens are Ti-saturated because of the presence of ilmenite (or rutile), it would appear that the changes in Ti content of the two micas as a function of metamorphic grade represent temperature-dependent changes in the Ti saturation limits of biotite and muscovite. The two parallel trends shown on Figure 3 for rutile-bearing specimens probably reflect such a T-dependent change in the Ti-saturation limit of biotite. The experimental work of Robert (1975) has also shown an extension of the Ti-saturation limit of biotite (phlogopite) as a function of T.

Table 3A. Intermediate Mg/Fe biotites from the Rangeley quadrangle, arranged in order of Mg/Fe ratio. Staurolite to Lower Sillimanite Zone. See Guidotti (1974) for complete analyses.

	Formulas Based on 22 Oxygen												
	a96	b41	a28	a95	a36	b95	a52	a72	a8	a33	a88	a58	Ave.
IV Si	5.32	5.28	5.38	5.34	5.32	5.32	5.38	5.38	5.38	5.36	5.38	5.38	5.35
Al	2.68	2.72	2.62	2.66	2.68	2.68	2.62	2.62	2.62	2.64	2.62	2.62	2.65
VI Al	.92	.86	.92	.94	.82	.88	.94	.88	.92	.90	1.00	.92	.908
Ti^{4+}	.18	.20	.20	.20	.18	.18	.18	.18	.18	.20	.20	.18	.188
Fe^{2+}	2.76	2.68	2.62	2.58	2.66	2.58	2.50	2.52	2.48	2.38	2.42	2.32	4.735
Mg	1.98	2.10	2.06	2.06	2.24	2.18	2.18	2.24	2.22	2.30	2.38	2.38	
Mn^{2+}	.01	.012	.008	.008	.006	.014	.008	.01	.006	.01	.012	.008	
Zn	-	.006	.002	.006	.002	.002	.006	.004	.004	.002	-	-	
Σ	5.85	5.858	5.81	5.794	5.908	5.836	5.814	5.834	5.81	5.792	6.012	5.808	5.844
XII K	1.58	1.64	1.62	1.64	1.60	1.62	1.56	1.58	1.64	1.62	1.64	1.60	1.61
Na	.10	.10	.10	.10	.08	.08	.12	.10	.068	.10	.08	.10	.094
Ca	.006	.002	-	-	.004	.002	-	-	.002	.002	.006	.002	
Ba	.002	.002	.002	.002	.002	.002	.002	.002	.002	.002	.002	.002	
Σ	1.688	1.744	1.722	1.742	1.686	1.704	1.682	1.682	1.712	1.724	1.728	1.704	
ΣAl	3.60	3.58	3.54	3.60	3.50	3.56	3.56	3.50	3.54	3.54	3.62	3.54	3.557
Mg/Fe	.717	.784	.786	.798	.842	.845	.872	.889	.895	.966	.983	1.026	
$r(m)^{VI*}$	.72	.72	.71	.71	.72	.71	.71	.71	.71	.71	.71	.71	

*Room temperature values (A) based upon cation sizes given in Shannon and Prewitt (1969, 1970).

Table 3B. Mg-rich biotites from Upper Staurolite to Lower Sillimanite Zone specimens of the Smalls Falls Formation in the northern portion of the Rumford 15' quadrangle. See Guidotti *et al.* (1975b) for the complete analysis.

	Formulas Based on 22 Oxygen								
	e28a	e28b	D24	e31	e26	e25	e32	G24	Ave.
IV Si	5.583	5.560	5.648	5.617	5.634	5.710	5.568	5.681	5.625
Al	2.417	2.440	2.352	2.383	2.366	2.290	2.432	2.319	2.375
VI Al	0.982	0.908	0.877	0.900	0.924	0.871	0.859	0.879	.900
Fe^{2+}	1.146	1.133	.971	.928	0.716	0.569	0.565	0.294	4.87
Mg	3.583	3.695	3.901	3.960	4.154	4.335	4.423	4.622	
Mn^{2+}	.036	.030	.037	.024	.028	.024	.033	.021	
Ti^{4+}	.106	.112	.091	.081	.070	.062	.069	.055	.081
Σ	5.853	5.878	5.877	5.893	5.892	5.861	5.949	5.871	5.884
XII K	1.455	1.491	1.482	1.475	1.454	1.508	1.474	1.528	1.483
Na	.063	.059	.055	.059	.062	.067	.061	.062	.061
Ca	.000	.000	.000	.000	.000	.000	.000	.000	
Σ	1.518	1.550	1.537	1.534	1.516	1.575	1.535	1.590	1.544
ΣAl	3.399	3.348	3.229	3.283	3.290	3.161	3.291	3.188	3.275
Mg/Fe	3.126	3.261	4.018	4.267	5.802	7.619	7.828	15.721	
$r(m)^{VI}$*	.70	.70	.70	.70	.70	.70	.70	.69	

*Room temperature values (A) based upon cation sizes given in Shannon and Prewitt (1969, 1970).

(2) K_D as a function of metamorphic grade

Because the observed change of K_D is small (0.224 to 0.280) and appears to occur only over the range from the upper staurolite zone to the lower sillimanite zone, some questions may exist as to its reality. However, Kwak (1968) has also recorded a change of this K_D over approximately the same range of metamorphic grades.

Assuming that the small change is real, it appears that temperature is the cause. Moreover, from our previous discussion it is then apparent that the Ti saturation limit of muscovite changes by a different amount than does that of biotite. It is unlikely that the moderate decrease of the average biotite Mg/Fe ratio (0.8590 to 0.8218, see Table 1) from the staurolite to the lower sillimanite zone could control K_D. Moreover, the effect would be in the wrong direction, since K_D decreases as biotite Mg/Fe ratio decreases.

(3) Relationship between K_D and Mg/Fe ratio of biotite

The relationship between K_D and Mg/Fe ratio of biotite appears to be influenced largely by the decrease of Ti in Mg-rich biotite, rather than to changes of Ti in the coexisting muscovite. The changes in biotite Mg/Fe ratio (for a given metamorphic grade) are controlled by the Mg/Fe ratio of the rock bulk composition and/or the mineral assemblage (*i.e.*, they are controlled by petrologic factors). Especially important in this context is the fact that all biotites considered are Si, Al, and Ti saturated. Thus, at a given metamorphic grade, changes such as variation of the Ti content must be the result of changes in the

Table 3C. Mg-rich biotites from the Upper Sillimanite Zone, Smalls Falls Formation, southwestern portion of the Rumford 15' quadrangle. See Guidotti *et al.* (1975b) for the complete analyses.

	Formulas Based on 22 Oxygen						
	7/16/73	P18b	P18a	P19	G57	P20	Ave.
IV Si	5.502	5.549	5.535	5.569	5.612	5.581	5.558
Al	2.498	2.451	2.465	2.431	2.388	2.419	2.442
VI Al	0.855	0.852	0.914	.902	.935	0.941	.8998
Fe^{2+}	1.356	1.228	1.091	0.913	0.825	0.613	4.68
Mg	3.298	3.447	3.517	3.790	3.873	4.109	
Mn^{2+}	.041	.034	.043	.052	.055	.049	
Ti^{4+}	.182	.168	.162	.131	.099	.106	.141
Σ	5.732	5.729	5.727	5.788	5.787	5.818	
XII K	1.728	1.730	1.712	1.617	1.580	1.566	1.655
Na	.084	.073	.062	.072	.098	.065	.076
Ca	.000	.000	.000	–	–	.000	
Σ	1.812	1.803	1.774	1.689	1.678	1.631	
ΣAl	3.353	3.303	3.379	3.333	3.323	3.360	3.342
Mg/Fe	2.432	2.807	3.224	4.151	4.694	6.703	
$r(m)^{VI}$*	.70	.70	.70	.70	.70	.69	

*Room temperature values (A) based upon cation sizes given in Shannon and Prewitt (1969, 1970).

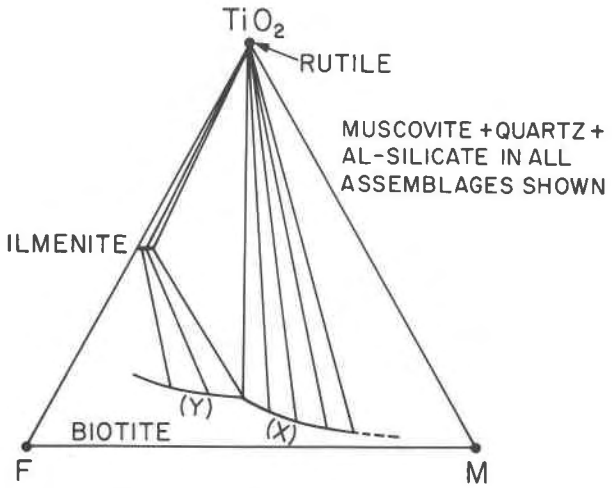

Fig. 4. Schematic projection from Al_2SiO_5 on to the Ti FM plane showing the change in the biotite Ti saturation limit in relation to change in the biotite Mg/Fe ratio and Ti-saturation phase. The break in slope of the biotite Ti saturation limit is hypothetical. (X) = Biotites from the Small's Falls Formation; (Y) = Other biotites.

petrologically controlled Mg/Fe ratio of biotite. On the other hand, other workers (*e.g.,* Dahl, 1970; and Dallmeyer, 1974a,b) argue that the Ti content controls the biotite Mg/Fe ratio and the Mg/Fe distribution coefficient between biotite and other Fe–Mg phases, especially garnet. We feel that the Mg/Fe ratio is more important in determining the chemistry of biotite, because of the magnitude of its range of variation and thus its effect on lattice dimensions.

For example, inspection of Table 1 shows (excluding specimens from Small's Falls Formation) that increase of Ti in biotite has no effect on the Mg/Fe distribution coefficient between muscovite and biotite. The radical decrease of Ti in biotite from the Small's Falls Formation does coincide with a decrease in this distribution coefficient. However, two factors suggest that this is not caused by the decrease of Ti in biotite: (a) The decrease in biotite Ti is very small *compared* to the change in biotite Mg/Fe ratio. (b) The mineral assemblages in the Small's Falls specimens are similar to the other specimens only in the sense of being Al-, Ti-, and Si-saturated. For example, they lack both staurolite and garnet, but commonly contain cordierite. These differences may explain the change in the Mg/Fe distribution between muscovite and biotite rather than changes of Ti in biotite.

The inverse relation between biotite Mg/Fe ratio and Ti content raises two basic questions. The first concerns the availability of Ti to enter the micas and the inverse trends of Ti contents in muscovite and biotite—*i.e.,* why should muscovite show a slight enrichment in Ti, whereas biotite is notably depleted? The second question is how a marked increase of biotite Mg/Fe inhibits substitution of Ti into biotite.

With regard to the relative availability of Ti, it should be noted that all specimens with high K_D have several characteristics in common. Most importantly, they all have abundant modal sulfide (commonly up to 5 to 10 modal percent). Guidotti (1970) has pointed out that an increase of sulfides in pelitic schists produces several effects, such as subtracting Fe^{2+} from the silicate and oxide phases. We have found that as modal sulfide increases (*e.g.,* > 1%): (1) Mg/Fe in biotite increases, and in rocks with 5–10 percent pyrrhotite, it reaches values as great as 15.7. (2) Muscovite increases modally, whereas biotite decreases modally. (3) Garnet decreases modally and is absent from rocks with greater than 2 to 3 percent sulfide. (4) Ilmenite decreases modally and becomes enriched in MnO, especially in rocks with no garnet. In rocks with more than 3–4 percent pyrrhotite, rutile is present instead of ilmenite (see Mallio and Gheith, 1972, for a similar observation). Phase-rule considerations discussed by Thompson (1972) provide an understanding of why only one, rather than both, of the Ti phases, rutile and ilmenite, is likely to be present in a given rock. (5) In specimens with 5 to 10 percent sulfide, cordierite can be found.

In simplified manner, these features can be ascribed to the abundant pyrrhotite taking up much of the available Fe^{2+}, thereby leaving a silicate bulk composition enriched in components such as MgO, K_2O, TiO_2, *etc.* Of the 117 coexisting muscovite–biotite pairs considered in this study, 20 show the above effects (see Guidotti, 1970, for further discussion of such sulfide–silicate phase relations). In view of points 1–5 listed above (especially #4), it is evident that as modal sulfide increases, Ti is released to concentrate in other minerals such as muscovite. Moreover, in highly sulfidic rocks that have rutile as the Ti phase it would seem likely that the activity of TiO_2 will be higher than in rocks with ilmenite. Hence, the Ti levels in the coexisting silicates would be expected to increase over the levels present in the ilmenite-bearing rocks. In summary, it is not unavailability of Ti that is causing the Ti decrease in biotite in rocks with high Mg/Fe biotite (*i.e.,* high sulfide rocks). In fact, the availability of Ti is greater in such rocks, as shown by the presence of rutile and the increase of Ti in the coexisting muscovite.

In order to postulate a model to explain how high Mg/Fe ratio inhibits substitution of Ti into biotite, it

is useful to consider two factors: (1) the sizes of the cations involved and, hence, the degree of fit between the tetrahedral and octahedral sheets, and (2) the necessity of charge balance. To this end several useful features emerge if the data concerning site occupancy for biotites with Fe > Mg (Table 3A) are compared against those for biotites with Mg >> Fe (Table 3B):

(1) Average Si increases and Al^{IV} decreases by 0.275.

(2) Average Ti decreases by 0.107.

(3) Average Al^{VI} undergoes very little change: 0.908 to 0.900. [From (1) and (3) it is evident that Al (total) decreases].

(4) The average number of *filled* octahedral positions increases from 5.84 to 5.88. Hence, there is essentially no change in the number of vacancies in going from the Fe to the Mg biotites.

(5) The average number of K atoms decreases by 0.127, and the average number of (Na+K) atoms decreases by 0.16.

These changes are summarized in Table 4. Although the observed numerical changes are small, it is important to note from Tables 3A and 3B that there is *no* overlap in the range of values within each group of samples.

To understand the inverse relationship between Ti content and Mg/Fe ratio in biotite, it is useful to emphasize (as done by Hazen and Wones, 1972) that the observed radical change in biotite Mg/Fe will have a marked effect on the lateral dimensions of the octahedral sheet. Tables 3A–3C show the decrease in the average size of the octahedrally-coordinated cations in going from moderate to high Mg/Fe ratios. These averages are based on cation sizes given by Shannon and Prewitt (1969, 1970) and represent room-temperature values. Radoslovich and Norrish (1962) have shown that the lateral dimensions of the octahedral sheet will be diminished in Mg-rich biotites, and that in phlogopite the $AlSi_3$ tetrahedral sheet is too large to fit directly on the Mg_3 octahedral sheet without some size adjustment of the tetrahedral sheet. As discussed by these authors, this size adjustment of the tetrahedral sheet is probably most readily accomplished by rotation of the tetrahedra within the plane of the tetrahedral sheet. This rotation is measured by an angle, α, which is a measure of the deviation of the arrangement of tetrahedra from hexagonal symmetry (see Fig. 8 of Hazen and Wones, 1972).

As developed by Hewitt and Wones (1975), increase of Al^{VI} and Al^{IV} in Mg-biotites will require even greater α rotation to achieve a fit between the tetrahedral and octahedral sheets of biotite. Indeed, they even suggest that limitations on how much tetrahedral rotation can occur serve to limit how much Al^{IV} and Al^{VI} can be present in an Mg-rich biotite. They indicate that a limit is reached on the amount of tetrahedral rotation possible when the K–O bond

Table 4. Summary of changes in site occupancy and resultant charge contribution between biotites of Tables 3A and 3B. [Sites per formula unit, $W_2^{XII}(X, Y)_6^{VI}(Z_8^{IV}O_{20})(OH)_2$].

Cations and Site Designation	Average of Biotites from Table 3A	Average of Biotites from Table 3B	Change in site occupancy	Resultant change in charge contribution by site
K in XII Sites	1.61	1.483	-.127	-.127
Occupied VI Sites	5.844	5.884	+.04	+.08*
Ti in VI Sites	.188	.081	-.107	-.214
(Mg + Fe) in VI Sites	4.735	4.87	+.135	-
Al in VI Sites	.908	.900	-.008	-.008
Al Total in (VI + IV) Sites	3.557	3.275	-.282	-
Si in IV Sites	5.35	5.625	+.275	+.275
				Σ = +.006

*Change in charge of VI sites due to change in number of vacancies in VI sites, assuming the change in vacancies involves only (Fe^{2+} + Mg).

lengths between the interlayer K and O's of the tetrahedral sheet become shortened to ~ 2.8 A ($\alpha \approx 14°$). Because substitution of the small Ti cation into the octahedral sheet also decreases its lateral dimensions, it is evident that the above suggested limitation on Al^{VI} in Mg-rich biotite could also apply to Ti, especially in an Al-rich, Mg biotite. Indeed, the effect of Ti on α could be enhanced, because of the probable concomitant substitution of Al^{IV} for Si^{IV} and its attendant *enlargement* of the tetrahedral sheet.

Calculation of the influence of Ti on tetrahedral rotations by means of the procedure outlined in Hewitt and Wones (1975) did result in α exceeding the values they suggested as upper limits. However, the validity of the procedure Hewitt and Wones have used to calculate α, which is based on earlier work by Donnay *et al.* (1964), is subject to question. We have tested this procedure on biotites for which α is known from X-ray structural determinations; the resulting correlation between the observed and calculated α could only be described as poor.

McCauley and Newnham (1971) have also presented an empirical method for calculating α. Although this method requires some idealizing of biotite formulas, one is able to reproduce closely the α's determined from X-ray structural studies for several biotites not used in the development of McCauley and Newnham's formula. Similar calculations for two Fe-rich biotites from Table 3A and two Mg-rich biotites from Table 3B give the following results;

	Mg/Fe	α
b41	0.7836	8.67°
b95	0.8450	9.88°
e28B	3.261	10.32°
e32	7.828	10.67°

In order to remain consistent with the procedure developed by McCauley and Newnham (1971), the ionic radii used in these calculations were taken from the *International Tables of X-ray Crystallography,* Vol. III. It should be noted that these calculated results represent room temperature and pressure values. If we take into account the effects of pressure and temperatue on cation–oxygen bond lengths as shown by Hazen (1975), the above α values decrease slightly, primarily due to expansion of the octahedral sheet relative to the tetrahedral sheet (*e.g.*, at 600°C and 4 kbar, the α value for specimen b41 becomes 7.38°). However, this calculation of the effect of pressure and temperature on α neglects any influence on the field strength term or the constant terms of McCauley and Newnham's formula.

To the extent that the above calculations are valid, they indicate an important point with regard to the biotites from northwestern Maine; α does not change greatly despite a large change of Mg/Fe. Moreover, the α's calculated for our samples are somewhat larger than those reported in the literature, the latter based upon actual structural determinations. Finally, it is important to realize that in the McCauley and Newnham calculation procedure the Al^{IV}/Si ratio of a given biotite has a significant influence on the α obtained; decreasing Al^{IV} strongly reduces α.

In view of the results of our calculation of α and the fact that Figure 3 of Hazen and Burnham (1973) strongly suggests a maximum attainable value for α near 11°, it appears that—as suggested by Hewitt and Wones (1975)—there is an upper limit on the amount of tetrahedral rotation that can be employed to achieve size adjustment between the tetrahedral and octahedral sheets of biotite. If such a premise is accepted, it is possible to suggest an explanation for the observed inverse relationship between Ti and high Mg/Fe in Al-rich biotites, and also an explanation for the low Al^{IV} (*i.e.*, high Si) in these same biotites.

By increasing Si at the expense of Al^{IV} in high Mg/Fe, Al-rich biotites, the amount of tetrahedral rotation needed to obtain a fit between tetrahedral and octahedral sheets can be decreased—even though this rotation will be greater than for a corresponding Fe^{2+}, Al-rich biotite. Decrease of Ti in the octahedral sites should also contribute to a decrease of α, especially because such a decrease of Ti will, for charge-balance reasons, lead to a decrease of Al^{IV} (*i.e.*, increase of Si). Alternatively, one can ascribe the decrease of Ti in the octahedral sites to a charge balance control due to increase of Si in the tetrahedral sites for size adjustment reasons. The important point is that the Ti, Si, and Al^{IV} substitutions are exactly those required to achieve a better fit between the tetrahedral and octahedral sheets, and thus minimize the amount of tetrahedral rotation otherwise required by high Mg/Fe in an aluminous biotite. Substitution of Si for Al^{IV} would clearly serve as a means of shrinking the lateral dimensions of the tetrahedral sheets in biotites, thus facilitating a better fit with an Mg-rich octahedral sheet. The reverse substitution has, of course, commonly been invoked as a means of enlarging the tetrahedral sheets (Dallmeyer, 1974a,b; Hewitt and Wones, 1975).

Inasmuch as the model discussed above involves substitution of ions of different charges, it is impor-

tant to consider charge balance aspects in further detail. Several charge balance models have been proposed to account for replacement of X^{2+} by Ti (Foster, 1960). One of these is:

$$(1)\quad (X^{2+})^{VI} + (2\ Si^{4+})^{IV} \rightleftharpoons (Ti^{4+})^{VI} + (2\ Al^{3+})^{IV}$$

Other exchange models involving formation of octahedral vacancies can be devised, but the data presented above lend them no support.

The model given by equation (1) is augmented by Table 4 which shows the charge variations that must accompany the observed changes in site occupancy. The charge contribution from the increase of Si is close to balancing the decrease attributable to Ti decrease, as required by the substitutional model given in equation (1). Indeed, a very close approximation to charge balance is maintained by the substitutions observed to occur in the change from the Fe to Mg-rich biotites of Tables 3A and 3B, respectively.

Although the above model for explaining the decrease of Ti in Mg-rich, Al-saturated biotites seems to be internally consistent, it should be reemphasized that it depends on two assertions: (1) there is some upper limit on the amount of tetrahedral rotation ($\sim 11°$?) possible in biotites and (2) the decrease of Al^{IV} (increase of Si) and decrease of Ti in Mg, Al-rich biotites occurs in order to achieve lateral fit of the tetrahedral and octahedral sheets. Moreover, in this model, some aspect of a charge balance argument may be involved, but this is not separable from strictly structural considerations.

A great need is evident on the part of crystal chemists to check further the reliability of the methods used to calculate tetrahedral rotation angles. It is also very important to establish the maximum rotation possible in biotite and to relate α to the compositional variation of *common* rock-forming biotites.

An important implication of the model developed in this paper is that the amount of Ti that can enter biotite depends greatly on the amount of Al in the environment. Because high Al^{VI} in Mg biotites tends to increase the misfit between the octahedral and tetrahedral sheet, the compensating substitutions involve a decrease of Ti. By way of contrast, some *low*-Al phlogopites reported in the literature are extremely rich in Ti (*e.g.*, Table 7 of Dawson *et al.*, 1970). Once again, these observations demonstrate the influence of bulk composition and assemblage on the composition of a mineral. Clearly, one should not talk of the influence of intensive parameters on the composition of a mineral (*e.g.*, Ti in biotite) except in the context of the same or comparable mineral assemblage; *e.g.*, all specimens Al-, Ti-, and Si-saturated as in this study.

It should also be noted that because K_D is a function of the Mg/Fe ratio of the biotite, then the distribution of Ti between coexisting muscovite and biotite does not follow the Nernst Distribution Law over the whole range of biotite Mg/Fe ratio.

Acknowledgments

The writers express appreciation to S. W. Bailey, E. S. Grew, D. A. Hewitt, S. W. Lonker, and D. R. Wones for critical reviews of this paper. Their comments and suggestions have been a great aid to the writers. NSF Grant Ga-42834 (to C. V. G.) has provided support for much of the work.

References

Albee, A. L. (1965) Distribution of Fe, Mg, and Mn between garnet and biotite in natural mineral assemblages. *J. Geol., 73,* 155–164.

Cheney, J. T. (1975) *Mineralogy and Petrology of Lower Sillimanite through Sillimanite + K-feldspar Zone Pelitic Schists, Puzzle Mountain Area, N. W. Maine.* Ph.D. Thesis, University of Wisconsin, 291 p.

Dahl, O. (1970) Octahedral titanium and aluminum in biotite. *Lithos, 3,* 161–166.

Dallmeyer, R. D. (1974a) The role of crystal structure in controlling the partitioning of Mg and Fe between coexisting garnet and biotite. *Am. Mineral., 59,* 201–203.

——— (1974b) Metamorphic history of the northeastern Reading Prong, New York and northern New Jersey. *J. Petrol., 15,* 325–359.

Dawson, J. B., D. G. Powell, and A. M. Reid (1970) Ultrabasic xenoliths and lava from the Lashaine Volcano, Northern Tanzania. *J. Petrol., 11,* 519–548.

Donnay, G., J. D. H. Donnay, and H. Takeda (1964) Trioctahedral one-layer micas. II. Prediction of the structure from composition and cell dimensions. *Acta Crystallogr., 17,* 1374–1381.

Evans, B. W. and C. V. Guidotti (1966) The sillimanite–potash feldspar isograd in western Maine, U.S.A. *Contrib. Mineral. Petrol., 12,* 25–62.

Foster, M. D. (1960) Interpretation of the composition of trioctahedral micas. *U.S. Geol. Surv. Prof. Pap., 354-B,* 11–46.

Guidotti, C. V. (1970) The mineralogy and petrology of the transition from the lower to upper sillimanite zone in the Oquossoc area, Maine. *J. Petrol., 11,* 277–336.

——— (1973) Compositional variation of muscovite as a function of metamorphic grade and assemblage in metapelites from N.W. Maine. *Contrib. Mineral. Petrol., 42,* 33–42.

——— (1974) Transition from staurolite to sillimanite zone, Rangeley quadrangle, Maine. *Bull. Geol. Soc. Am., 85,* 475–490.

———, J. T. Cheney and P. D. Conatore (1975a) Coexisting cordierite + biotite + chlorite from the Rumford quadrangle, Maine. *Geology, 3,* 147–148.

———, ——— and ——— (1975b) Inter-relationship between Mg/Fe ratio and octahedral Al content in biotite. *Am. Mineral., 60,* 849–853.

Hazen, R. M. (1975) *Effects of Temperature and Pressure on the Crystal Physics of Olivine.* Ph.D. Thesis, Harvard University, 264 p.

——— and D. R. Wones (1972) The effect of cation substitution on the physical properties of trioctahedral micas. *Am. Mineral., 57,* 103–125.

——— and C. W. Burnham (1973) The crystal structures on one-layer phlogopite and annite. *Am. Mineral., 58,* 889–900.

Hewitt, D. A. and D. R. Wones (1975) Physical properties of some synthetic Fe–Mg–Al trioctahedral biotites. *Am. Mineral., 60,* 854–862.

Kwak, T. A. P. (1968) Ti in biotite and muscovite as an indication of metamorphic grade in almandine amphibolite facies rocks from Sudbury, Ontario. *Geochim. Cosmochim. Acta, 32,* 1222–1229.

Mallio, W. J. and M. A. Gheith (1972) Textural and chemical evidence bearing on sulfide–silicate reactions in metasediments. *Mineral. Deposita, 7,* 13–17.

McCauley, J. W. and R. E. Newnham (1971) Origin and prediction of ditrigonal distortions in micas. *Am. Mineral., 56,* 1626–1638.

Radoslovich, E. W. and K. Norrish (1962) The cell dimensions and symmetry of layer lattice silicates. I. Some structural considerations. *Am. Mineral., 47,* 599–616.

Robert, J. L. (1975) An experimental study of phlogopite solid solutions in the system K_2O–MgO–Al_2O_3–SiO_2–H_2O. Solubility of titanium in phlogopite solid solutions. *Geol. Soc. Am. Abst. with Programs, 6–7,* 844–845.

Shannon, R. D. and C. T. Prewitt (1969) Effective ionic radii in oxides and fluorides. *Acta Crystallogr., B25,* 925–946.

——— and ——— (1970) Revised values of effective ionic radii. *Acta Crystallogr., 26,* 1046–1048.

Thompson, J. B. (1972) Oxides and sulfides in regional metamorphism of pelitic schists. *24th Int. Geol. Congress (Montreal), Section* 10, 27–35.

Manuscript received, April 8, 1976;
accepted for publication, December 23, 1976